Research Article | Vol. 28, No. 23 / 9 November 2020 / Optics Express 34255
Optics EXPRESS

High pulse energy fibre laser as an excitation source for photoacoustic tomography

THOMAS J. ALLEN,[1,*] MARTIN BERENDT,[2] DI LIN,[2] SHAIFUL U. ALAM,[2] NAM T. HUYNH,[1] EDWARD ZHANG,[1] DAVID J. RICHARDSON,[2] AND PAUL C. BEARD[1]

[1]*Department of Medical Physics and Biomedical Engineering, University College London, Gower Street, WC1E6BT, UK*
[2]*Optoelectronics Research Centre, University of Southampton, Southampton, SO17 1BJ, UK*
[*]*t.allen@ucl.ac.uk*

Abstract: A custom fibre laser designed as an excitation source for biomedical photoacoustic tomography has been developed. It is based on a custom-drawn large core diameter fibre (200 µm) that enables high pulse energies (~10 mJ) to be achieved. The system can provide variable pulse durations (10 - 500 ns) and pulse repetition frequencies (100 Hz - 1 kHz), as well as arbitrary pulse bursts according to specific user defined sequences. The system is also compact and does not require external water cooling. This, along with the flexibility in the temporal characteristics of its output that it offers, will aid the translation of photoacoustic imaging to practical application in medicine and biology.

1. Introduction

Photoacoustic signals are typically generated using Q-switched Nd:YAG pumped OPO, Ti:sapphire or dye laser systems, as they can provide the necessary mJ pulse energies, nanosecond pulse durations and tunability in the visible and NIR wavelength range for biomedical photoacoustic tomography [1]. These systems have been used widely to obtain high quality photoacoustic images of tissue structures and have been instrumental in demonstrating the feasibility of the technique in the laboratory. However, they present several practical limitations due, in part, to their reliance on high pulse energy (> 100 mJ) Q-switched lasers as pump sources. These are typically of large physical size, a consequence of their low electrical-to-optical conversion efficiency which necessitates the use of bulky power supplies and external water-cooling units. In addition, they require regular maintenance, provide low pulse repetition frequencies (<200 Hz) thus limiting image frame rate and offer limited opportunity to control the pulse duration, shape and spacing. The latter inhibits the practical implementation of techniques such as photoacoustic flowmetry [2] or thermometry [3,4], the use of novel coded excitation schemes [5,6] and the study of the time-dependent photoacoustic generation process.

Fibre laser technology can potentially overcome these limitations, allowing compact, reliable and efficient pump sources to be developed. The long length and small core diameter of the fibre gain medium provides for high gain, low laser thresholds and high gain efficiencies. This, in combination with the high efficiency of high-power pump laser-diodes allows high electrical-to-optical conversion efficiencies to be achieved thereby obviating the need for bulky high voltage power supplies. In addition, the high surface area-to-volume ratio of the gain medium provides for efficient heat dissipation without the need for external water cooling. Moreover, the fiberized nature of the laser cavity eliminates the need for careful alignment of free space components, allowing for reliable, robust and compact system designs. Fibre lasers are not only advantageous

#401708 https://doi.org/10.1364/OE.401708
Journal © 2020 Received 1 Jul 2020; revised 11 Sep 2020; accepted 1 Oct 2020; published 28 Oct 2020

Optics EXPRESS

in terms of their practical utility, but also in their functionality. The Master Oscillator Power Amplifier (MOPA) configuration, which uses a chain of fibre amplifiers to amplify the output of a seed laser, provides an output that can be arbitrarily modulated over a very wide range of timescales (sub ps - ms). This enables the pulse repetition frequency (PRF), pulse duration and shape to be varied arbitrarily allowing the implementation of a wide variety of photoacoustic excitation schemes. Semiconductor devices such as laser diodes [7] or light emitting diodes [8] (LED) can provide comparable flexibility in their temporal output and have been used as photoacoustic excitation sources but are limited by their relatively low pulse energy, a couple of mJ or less for laser diodes and a few hundred of µJ for LEDs.

To date, fibre laser systems have been developed mostly for material processing (e.g., welding, drilling or engraving) for which high average powers (rather than high pulse energies) and excellent beam quality are the primary requirements. Although pulsed fibre lasers have previously been used for optical resolution photoacoustic microscopy [9] (OR-PAM) as they can provide the required high beam quality (M^2<1.2), modest pulse energies (< 1 µJ) and high PRF (> 100 kHz) as well as access to visible wavelengths when frequency doubled, they have rarely been used for widefield photoacoustic tomography [10,11]. This is largely due to fibre lasers providing insufficiently high pulse energies, typically ~1 mJ or less, due to the small core diameter (<25 µm) fibres which are employed to achieve a high quality beam. However, for photoacoustic tomography, a high beam quality is not a requirement. Hence there is scope to increase the pulse energies and peak powers by using large core diameter fibres [12,13], which are able to amplify pulses to high energy (tens of mJ) and mitigate intensity related nonlinearities such as stimulated Brillouin scattering (SBS) and stimulated Raman scattering (SRS).

In this study, we have developed a novel fibre laser system based on a MOPA architecture that was designed specifically for photoacoustic tomography. A distinctive feature of the system is that it employs a custom drawn large core diameter fibre in the power amplifier stage. This provides the necessary high peak power handling to permit the generation of mJ scale pulse energies with nanosecond pulse durations as required for photoacoustic tomography. An additional novel aspect of the design is that the linewidth of the laser output was kept narrow (~0.2 nm). This is required as ultimately our goal is to combine this fibre laser with an Optical Parametric Oscillator (OPO) in order to obtain a wavelength-tuneable excitation source for photoacoustic tomography. A narrow linewidth is required for maximizing the frequency conversion process.

The manuscript is structured as follows; a detailed description of the laser architecture is provided in section 2, its suitability as an excitation source for 3D in-vivo photoacoustic imaging is demonstrated in section 3, and section 4 discusses its pulse shaping capabilities and experimentally illustrates the implementation of two distinct concepts: the ability to control the bandwidth of the generated photoacoustic signal by varying the duration or spacing of the excitation pulses and the ability to implement a coded excitation scheme by generating complex sequences of pulses.

2. High pulse energy fibre laser

2.1. Overview

The design of the fibre laser is based on a MOPA configuration, which involves amplifying the optical output of a seed source using a chain of five Ytterbium-doped fibre amplifiers. To scale up the optical power, the core diameters of the fibre amplifiers were successively increased, 6 µm, 10 µm, 25 µm, 50 µm and 200 µm, and had, respectively, a saturation energy of 16 µJ, 44 µJ, 275 µJ, 1.1 mJ and 17.6 mJ. For a 200 µm core diameter fibre, this corresponds to a theoretical extractable energy of 176 mJ. Figure 1 shows a schematic of the fibre laser which can be described in three parts. The first part is the seed and pre-amplifier stage which provides the optical input to the subsequent amplifier stages with the desired linewidth, wavelength, PRF and pulse shape and duration. The second part comprises a chain of three power amplifiers used to further increase the seed energy. Using three amplifiers with increasing energy gain, as opposed

Optics EXPRESS

to a single one, minimises any distortion of the pulses due to gain saturation. The third part of the system, comprised a custom 200 µm core diameter fibre to allow the output pulse energy to be increased to 10 mJ.

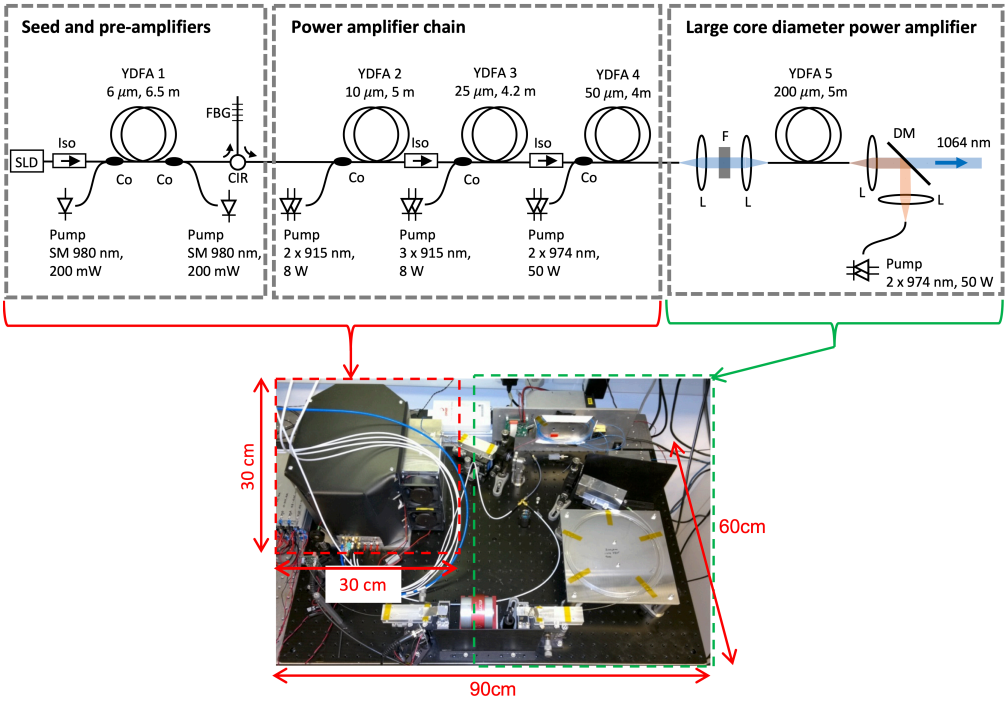

Fig. 1. Schematic of the high pulse energy fibre laser (SLD: super luminescent diode, Co: coupler, CIR: circulator, FBG: Fibre Bragg Grating, YDFA: Ytterbium doped fibre amplifier, Iso: fibre optic isolator with integrated band pass filter, L: lens, F: free-space filter, DM: dichroic mirror, SM: single mode).

2.2. *Seed and pre-amplifier*

The aforementioned chain of fibre amplifiers was seeded using a Super Luminescent Diode (SLD), which had a central wavelength of 1064 nm, a 3 dB linewidth of 20 nm and a peak power of ~200 mW. As opposed to a conventional Fabry–Pérot laser diode, a SLD provides a smooth and broad output spectrum which is independent of the input pulse parameters. This allows arbitrary shaping of the directly modulated output of the SLD without generating excessive stimulated Brillouin scattering (SBS). The latter is often associated with directly modulated Fabry–Pérot laser diode seed sources, due to their narrow linewidth, which not only can lead to severe distortions of the output pulse shape, but can also damage the fibre laser due to the strong back-propagating Brillouin signal. As ultimately the aim is to frequency double the output to 532 nm in order to pump an OPO to provide the required tunability for photoacoustic tomography, the SLD output was filtered down to a 0.2 nm 3 dB spectral width. This linewidth is narrow enough to provide highly efficient frequency conversion, while remaining broad enough to mitigate the effects of SBS. The filtering was implemented using an optical circulator and a Fibre Bragg Grating (FBG) and produced the desired spectral width but reduced the optical power by 20 dB. To compensate for this loss, a pre-amplification stage (YDFA 1) was incorporated between the seed and the filter. This first amplifier used a 6.5 m long polarisation maintaining (PM) Ytterbium-doped fibre with 6 µm core diameter and was core-pumped using two 980 nm single

Optics EXPRESS

mode laser diodes configured in forward and backward pump configurations, each providing 200 mW of pump power. The gain of the amplification stage was ~25 dB and the output pulse energy was 2.5 μJ for a 40 ns pulse duration at 100 Hz PRF. The SLD was driven by an arbitrary waveform generator (AWG) and could provide pulse durations ranging from 10 ns to 500 ns. To achieve rectangular optical pulses at the output of the fibre laser, the electrical pulses used to drive the SLD were pre-shaped (e.g., their leading edge was made lower than their trailing edge) to compensate for the effects of gain saturation, which causes the trailing edge of the pulse to experience a lower gain than the leading edge as it propagates through the chain of fibre amplifiers.

2.3. Power amplifier chain

The output of the seed stage was amplified by a chain of three pre-amplifiers (YDFA 2, YDFA 3 and YDFA 4) with a net overall gain of ~23.4 dB, providing an output pulse energy of 550 μJ. All three amplifiers were cladding pumped, allowing the use of high-power multimode laser diodes. YDFA 2 used a 5 m long PM Ytterbium-doped fibre with a 10 μm core diameter and was pumped using two 915 nm laser diodes each providing 8 W of output power. YDFA 3 used a 4.2 m long PM Ytterbium-doped fibre with a 25 μm core diameter and was pumped using three 915 nm laser diodes each providing 8 W output power. YDFA 4 used a 0.85 m long custom drawn (in house) PM Ytterbium-doped fibre with a large core diameter (50 μm) and was pumped using a 975 nm laser diode providing 50 W output power. The amplifier stages were pulse-pumped to avoid pumping the fibre over long periods of time when no input signal was present, which would otherwise generate excessive Amplified Spontaneous Emission (ASE) and compromise the signal amplification. To protect against back reflections and remove any generated ASE, fibre optic isolators with integrated band pass filters (10 nm at 3 dB) were placed between each amplifier stage.

2.4. Large core diameter power amplifier

The final amplification stage (YDFA 5) provided a gain of ~12 dB and used a 5 m long custom drawn (in house) Ytterbium-doped fibre. The fibre had a D-shaped cladding with 690 μm diameter and a step index core with 200 μm core diameter. The Yb concentration was estimated to be 1.3×10^{26} ions/m^3 from absorption measurements and the numerical aperture (NA) of the fibre was ~0.14. The fibre was coated with a low index polyimide, to enable it to be cladding pumped using four 60 W 975 nm laser diodes (operated in pulsed mode) in a backward configuration. Free-space optics were used in this stage of the system as passive components such as fibre isolators and pump/signal combiners are not commercially available for such large core diameter fibre. The output of the power amplifier chain was coupled into the 200-μm-core-diameter fibre through a pair of lenses between which a band pass filter is inserted to remove out of band ASE. The final system was able to provide a maximum pulse energy of 10 mJ, variable pulse durations (10 to 500 ns) and pulse repetition frequencies (100 Hz to 1 kHz). The laser system was designed such that a near constant pulse energy could be provided, independently of pulse duration and pulse repetition frequency. A long-term stability test was carried out when operating at an average power of 2 W with a 20 ns pulse duration, a 200 Hz PRF and a pulse energy of 10 mJ. The output pulse energy was stable with only a variance of +/−0.1 mJ while running for 50 minutes. The linewidth of the laser was measured at its output to be 0.25 nm FWHM, with an OSNR ranging from 21 dB to 17 dB, for 5 mJ to 10 mJ operation. No spectral features from nonlinear interactions were seen or expected due to the large core diameters of the fibres.

A photograph of the system is shown in Fig. 1. The seed and first four amplifier stages occupy a footprint of 25 cm × 30 cm × 30 cm. The final high power amplifier stage was laid out on the remaining space of a 60 cm × 90 cm bread board; ultimately, it will be replaced by a polarisation maintaining fibre of equivalent core diameter and spliced to the rest of the

Optics EXPRESS

system – we have already reported single polarisation MOPA operation using the current non-PM 200-µm-core-diameter fibre using a bi-directional final stage amplifier configuration [14]. This will allow the entire system to be fully fiberized and housed in a relatively compact (30 cm × 30 cm × 30 cm) unit. This is enabled in part by the fact that the fibre laser system does not require water cooling.

3. In-vivo photoacoustic imaging

The fibre laser was combined with a photoacoustic imaging system to obtain 3D images of the superficial vasculature in a human hand. The imaging system is illustrated in Fig. 2(a); it uses an optical ultrasound sensor based upon a Fabry–Perot polymer film interferometer to detect the acoustic signals [15]. The Fabry Perot sensor is composed of a 22 µm thick polymer film sandwiched between two dichroic mirrors. These mirrors are highly reflective (>95%) between 1500 and 1650 nm, but highly transmissive between 600 nm and 1200 nm. This allows the optical pulses emitted by the fibre laser (1064 nm) to be transmitted through the sensor, into the underlying tissue where they are absorbed, generating photoacoustic waves. The latter then propagate back to the sensor, modulating the optical thickness of the Fabry–Perot interferometer and hence its reflectivity. The sensor is read out by scanning focused interrogation laser beams [16] at 1550 nm over its surface and measuring the reflected light. From the 2D distribution of the photoacoustic waves, a 3D image is formed using a time reversal image reconstruction algorithm [17].

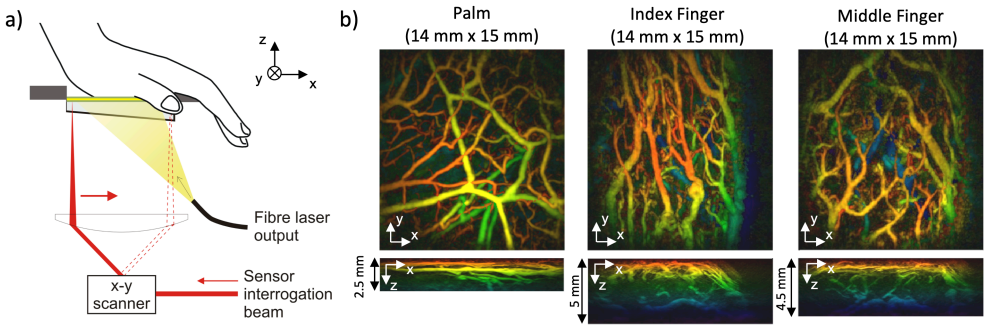

Fig. 2. In-vivo photoacoustic tomography showing the superficial vasculature in the hand; (a) Schematic of the Fabry- Perot scanner (b) x-y and x-z maximum intensity projection (MIP) of 3D image data set, color coded for depth.

This system was used to acquire 3D images of the vasculature in the human palm and fingertips as shown in Fig. 2(b). All experiments were conducted with the approval of UCL Research Ethics Committee (Project ID: 1133/001). The photoacoustic signals were recorded over a 14 mm by 15 mm area in steps of 100 µm. To guide the light to the sample, the output of the laser was fibre coupled into a passive large core diameter (Ø 600 µm) fiber, whose tip was place approximately 4.5 cm away from the sample resulting in a 2 cm diameter laser beam being incident on the sample. The pulse energy emitted by the fibre laser was 9 mJ, the PRF was 200 Hz and the pulse duration was 20 ns. The incident fluence was less than 2.2 mJ/cm^2, which is well below the Maximum Permissible Exposure (MPE) for skin for a 200 Hz PRF and an exposure time below 30s. The maximum intensity projections of the reconstructed 3D images are shown in Fig. 2(b). These images show the subcutaneous vasculature up to a depth of approximately 5 mm illustrating that the laser output characteristics in terms of pulse energy and duration meet the requirements for acquiring high quality in vivo photoacoustic images. The acquisition time was 14 seconds, ten times faster than that what would be achieved using a standard 20 Hz Q-switched

Optics EXPRESS

laser. Increasing the PRF of the laser would allow the imaging time to be reduced, although the total exposure duration would need to be decreased to remain below the safe maximum permitted exposure for skin. For example, for the pulse energy and illumination area referred to above, increasing the PRF to 1 kHz would require the total exposure time to be kept below two seconds which is achievable with a fast imaging system [18,19].

4. Temporal pulse shaping capability

The ability to readily control the temporal parameters (e.g., pulse shape, duration and spacing) of the pulse emitted by the fibre laser provides new opportunities to investigate the physics of photoacoustic signal generation (e.g., stress or thermal confinement), control the photoacoustic signal bandwidth to optimise SNR and implement novel time-domain flowmetry [2] or temperature [3] measurement methods. To demonstrate this versatility, two different concepts were illustrated experimentally. The first exploited the ability of the fibre laser to vary the duration and spacing of the emitted pulses in order to control the bandwidth of the generated photoacoustic signal. The second, exploited the ability of the fibre laser to generate complex sequences of pulses in order to implement coded excitation schemes.

4.1. Photoacoustic bandwidth control

To illustrate the effect of changing the pulse duration on the bandwidth of the generated photoacoustic signal, single point measurements were made for three different pulse durations (20 ns, 100 ns and 250 ns), each with 9 mJ of pulse energy. The measurements involved using the fibre laser to illuminate a planar black absorber immersed in water and measuring the generated photoacoustic signals with a broadband ($f_{-3\,dB}$ = 40 MHz) Fabry–Pérot sensor. The absorber was located 5 mm above the sensor, and the diameter of the optical beam incident on the absorber was 20 mm. The optical pulses produced by the laser were measured using a photodiode with a −3 dB bandwidth of ~400 MHz and are shown in Fig. 3(a); the generated photoacoustic signals and their corresponding frequency spectra are shown in Figs. 3(b) and 3(c), respectively. As the pulse duration increases, the amplitude of the photoacoustic signals decreases and their temporal shape broadens. This is because the generated signal is the convolution of the pulse temporal profile with the signal that would be generated by an impulsive deposition of the laser energy. In the frequency domain, the increase in pulse duration corresponds to a narrowing of the bandwidth, resulting in a −3 dB bandwidth of 15 MHz, 5 MHz and 1.7 MHz for the signals generated by the 20 ns, 100 ns and 250 ns pulse durations respectively. It is therefore possible to control the bandwidth of the generated photoacoustic signal by tailoring the duration of the excitation pulse.

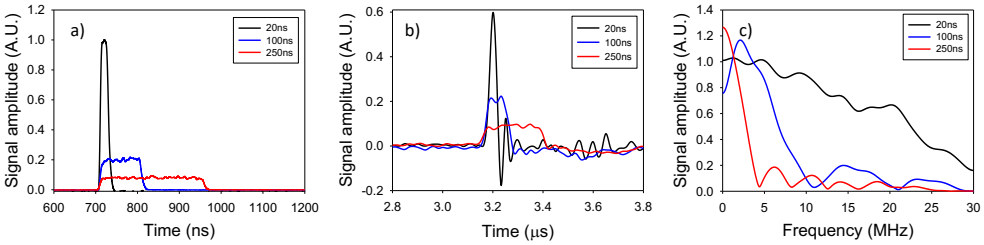

Fig. 3. Generation of photoacoustic signals in a planar black absorber using a range of pulse durations (20 ns, 100 ns and 250 ns); (a) optical pulses (b) and (c) show the generated photoacoustic signals and their frequency spectra respectively.

To demonstrate the effect of varying the pulse duration on reconstructed photoacoustic images, the palm of a hand was imaged using the experimental set-up shown in Fig. 2(a) using optical

Optics EXPRESS

pulses of different duration as shown in Fig. 3(a). The reconstructed images are shown in Fig. 4. It can be seen that, as the pulse duration increases, both the image resolution and contrast decrease. This is most evident in the image acquired with the 250 ns excitation pulse, where some of the smaller vessels (labelled A and B in the figure) visible in Figs. 4(a) and 4(b) can no longer be detected. The loss in resolution and contrast is a direct consequence of the decreasing bandwidth and amplitude of the signals when increasing the pulse duration. For the image obtained using a 100 ns excitation pulse duration [Fig. 4(b)], the deterioration in resolution and contrast compared to the image acquired using the 20 ns pulse duration is modest. This is because the pulse duration is not the dominant bandwidth limiting mechanism. In this particular case, the bandwidth is defined by the size of the acoustic sources (e.g., the diameter of the blood vessels) and the frequency dependent acoustic attenuation of biological tissue. The frequency response of the Fabry–Pérot sensor is sufficiently broadband (40 MHz at −3 dB) that it does not band-limit the detected photoacoustic signals. Therefore, in this case, increasing the pulse duration from 20 ns to 100 ns does not compromise image quality to a significant extent.

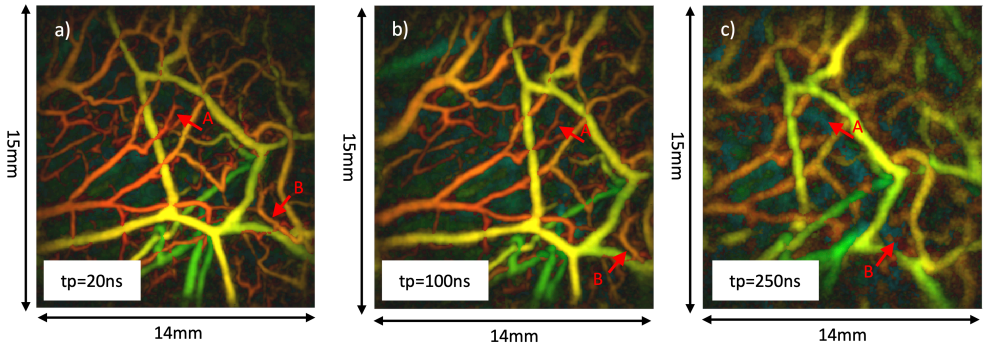

Fig. 4. Photoacoustic images of the palm of a human hand, generated with pulse durations of (a) 20 ns (b) 100 ns and (c) 250 ns. The images are color coded for depth.

Another example illustrating how the bandwidth of the generated photoacoustic signals can be controlled is shown in Fig. 5. As mentioned above, the experiment consisted of generating photoacoustic signals in a black planar absorber immersed in water and detecting them. Figure 5(a) shows a train of optical pulses generated by the fibre laser, where each pulse is 25 ns in duration, is of 2 mJ pulse energy and has a pulse-to-pulse separation of 250 ns. The resulting photoacoustic signal is shown in Fig. 5(b), and its frequency spectrum is shown in Fig. 5(c). In the time domain, it can be seen that a unipolar signal is generated for each of the optical pulses. In the frequency spectrum, this corresponds to delivering the optical energy in specific narrow

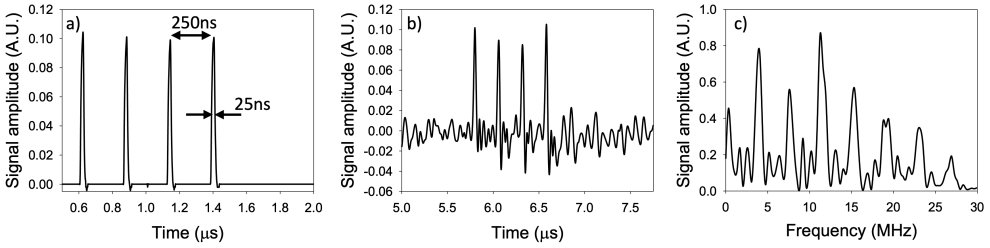

Fig. 5. Photoacoustic pulse train generation (a) optical pulses; (b) photoacoustic signals generated in a black absorber; (c) frequency spectrum of the signal shown in (b).

Optics EXPRESS

frequency bands (e.g., 4, 8, 12, 16, 20 and 24 MHz). The fundamental 4 MHz frequency band is defined by the spacing between pulses (1/250 ns) and the remaining frequency bands correspond to its harmonics.

Controlling the bandwidth of the generated photoacoustic signal using these approaches may, in some circumstances, be beneficial in terms of SNR as it provides a means of preferentially exciting specific frequency ranges that fall within the detector frequency response or avoid excessive acoustic attenuation in tissue [20].

4.2. Pulse sequences

The fibre laser can generate complex arbitrary sequences of pulses such as pseudo random binary sequences used in coded excitation schemes, which have been studied for improving SNR in peak power limited excitation systems [6,21–24] and wavelength multiplexing [5,8]. Coded excitation schemes rely on two binary sequences (e.g., sequence 1 and 2) whose cross-correlation is an impulse with a FWHM that corresponds to the widths of the pulses in the binary sequences (see Fig. 6). The first binary sequence (e.g., sequence 1) is used to generate a photoacoustic signal, and this signal is then cross-correlated with the second binary sequence (e.g., sequence 2) in order to obtain the photoacoustic signal which would have been generated using an impulse.

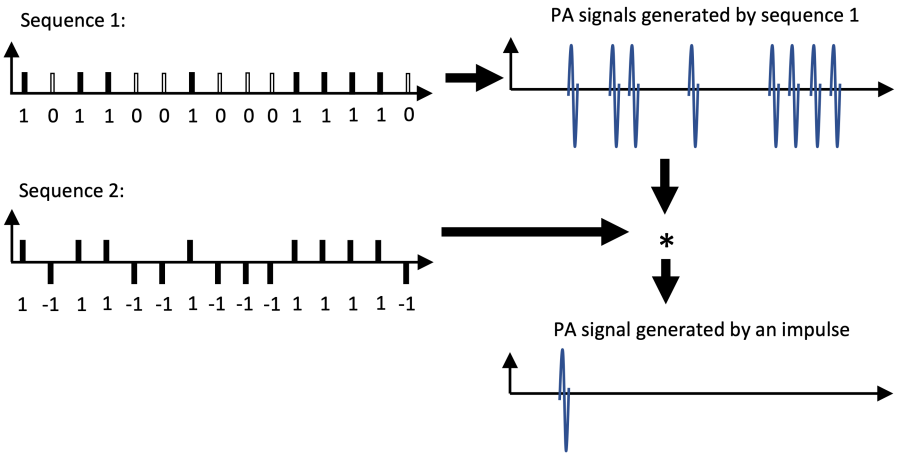

Fig. 6. Illustration of a coded excitation scheme.

The ability to implement these excitation schemes using the fibre laser was demonstrated using the experimental setup previously described, consisting of a black planar absorber immersed in water. The excitation sequence shown in Fig. 6 (sequence 1) was generated using the fibre laser and is shown in Fig. 7(a) where each of the 8 optical pulses forming the sequence was 25 ns long and of 1 mJ energy. The pulse-to-pulse separation within the sequence ranged from 250 ns to 1 µs; the entire sequence lasted 3.5 µs and was repeated at a repetition frequency of 200 Hz. The detected photoacoustic signals before and after cross correlation are shown in Figs. 7(b) and 7(c), respectively.

To demonstrate this approach for imaging purposes, the palm of a hand was imaged. For this, the Fabry–Pérot scanner shown in Fig. 2(a) was used to record the whole photoacoustic time series generated by the coded sequence shown in Fig. 7(a) for each scan point. The reconstructed photoacoustic image is shown in Fig. 8. The fibre laser could therefore be used as a prototyping tool to investigate the benefits of these excitation schemes over standard pulsed excitation methods.

Optics EXPRESS

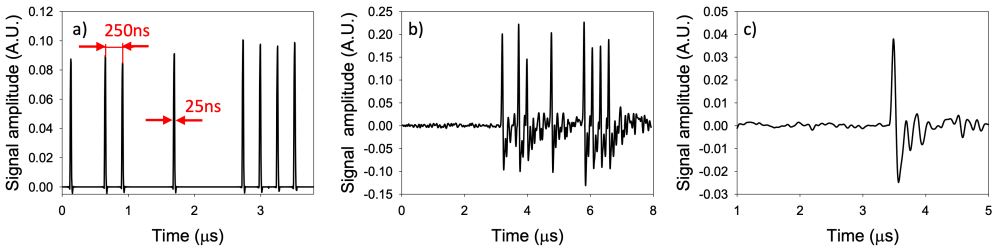

Fig. 7. Photoacoustic signals generated using a coded excitation scheme; (a) optical pulse sequence; (b) generated photoacoustic signal; (c) retrieved photoacoustic signal after cross-correlation.

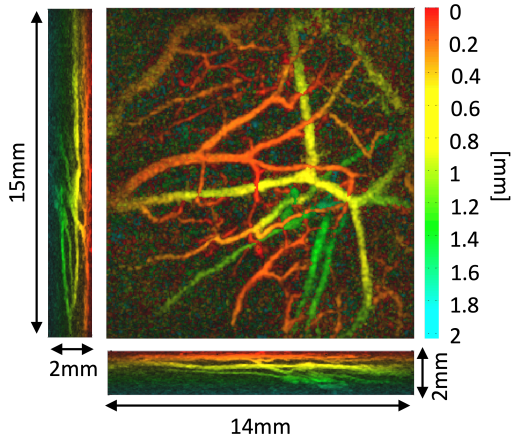

Fig. 8. Photoacoustic image of the palm of a hand obtained with the coded excitation scheme illustrated in Fig. 8 and the experimental setup shown in Fig. 2(a).

5. Discussion and conclusion

A novel, high pulse energy (> 10 mJ) fibre laser was developed for photoacoustic imaging applications. The system was compact, required no external water cooling, and the temporal characteristics of its optical output could be controlled by the user. Its pulse duration and PRF could be varied from 10 to 500 ns and 100 Hz to 1 kHz respectively, and arbitrary sequences of pulses generated. The system was shown to provide sufficiently high pulse energies and short enough pulse durations to enable the acquisition of high quality in-vivo photoacoustic images of the human hand.

The flexibility of the fibre laser in terms of the high degree of control that can be exercised over its temporal characteristics is a key distinguishing feature compared to fixed pulse duration Q-switched Nd:YAG based lasers commonly used for photoacoustic generation. This was demonstrated by (1) controlling the bandwidth of the generated photoacoustic signal by varying the duration or spacing of the excitation pulses and (2) implementing a coded excitation scheme by generating complex sequences of pulses. This flexibility makes the laser a versatile research tool for studying the physics of photoacoustic signal generation, for example to explore the relationship between the pulse temporal characteristics and thermal or stress confinement. In addition, it provides new opportunities for exploring the relationship between pulse shape and duration on image resolution and SNR. This is relevant to the use of sources which are peak power

Optics EXPRESS

limited, such as laser diodes and LEDs, as there is a known compromise between SNR and spatial resolution when adjusting the pulse duration; for example SNR can be enhanced by increasing pulse duration due to the increase in pulse energy but this is at the cost of resolution. The fibre laser could therefore be used as a prototyping tool to identify the optimum pulse characteristics in order to inform the operation of such sources. In a similar manner, the fibre laser could also be used to experimentally investigate the SNR-resolution trade-offs of laser systems such as the Alexandrite laser that provide relatively long pulse durations (> 50 ns). The ability to generate arbitrary pulse trains and sequences provides a means of evaluating novel coded excitation schemes designed to increase SNR or enable efficient multiplexing. It also enables the implementation of new signal processing schemes that require pulse sequences to provide additional functionality, for example photoacoustic thermometry [3] based on the non-linear response of the Grüneisen coefficient, photoacoustic flowmetry based on cross correlation techniques [2] or pump probe techniques [25] for recovering molecular information. Finally, for similar reasons, the system could be a valuable source for laser generated ultrasound sensing and imaging applications.

Although the imaging system discussed in this paper was shown to provide in-vivo images of the microvasculature with high contrast and resolution, it is limited to a single non-optimal excitation wavelength (1064 nm). However, the current system was designed with the intent to eventually frequency double its output in order to pump an OPO system, thereby providing tunability in the biologically relevant near infrared range (650 nm-900 nm). For this reason, the chain of fibre amplifiers was made using polarization maintaining fibres, and the linewidth of the system was kept narrow (~0.25 nm) to maximise frequency conversion efficiency. For such a fibre pumped OPO system to provide sufficient pulse energy (> 10 mJ) for practical photoacoustic tomography applications, the pulse energy provided by the fibre laser would need to be increased to overcome the losses incurred by the frequency conversion processes. This should be possible; a recent study [26] has demonstrated the feasibility of extracting 100 mJ out of a 200 µm core diameter fibre laser, although its broad linewidth (10 nm) and use of non-polarisation maintaining fibre would not permit efficient frequency conversion and therefore cannot be used to pump an OPO. In addition, that laser was limited to providing 10 ns pulses at a 10 Hz PRF without the pulse shaping capability provided by our system. One means of increasing the emitted pulse energy of our system would be to further scale up the pulse energy used to seed the last fibre amplifier, allowing for a larger portion of the energy stored within the large core diameter fibre to be extracted.

In summary, this work has shown that fibre lasers could be a realistic alternative to current excitation sources for biomedical photoacoustic tomography. Their compact size, reliability, efficiency and low maintenance, makes them well suited to operating in a clinical environment. Their high PRF (> 200 Hz) relative to standard Q-switched lasers (tens of Hz) enables faster photoacoustic image acquisition to be achieved. In addition, the flexibility in temporal output they offer makes them well suited to investigating and implementing novel time-domain signal processing techniques for enhancing image SNR and resolution and functionality. Future work will focus on further increasing pulse energy, and frequency doubling the output in order to pump an OPO system to access near-infrared wavelengths.

Funding

ERC (741149); Engineering and Physical Sciences Research Council (EP/J022144/1).

Disclosures

The authors declare that there are no conflicts of interest related to this article.

References

1. P. Beard, "Biomedical Photoacoustic Imaging," Interface Focus. **1**(4), 602–631 (2011).

Optics EXPRESS

2. J. Brunker and P. Beard, "Velocity measurements in whole blood using acoustic resolution photoacoustic Doppler," Biomed. Opt. Express **7**(7), 2789–2806 (2016).
3. Y. Zhou, M. Li, W. Liu, G. Sankin, J. Luo, P. Zhong, and J. Yao, "Thermal memory based photoacoustic imaging of temperature," Optica **6**(2), 198 (2019).
4. F. Gao, X. Feng, R. Zhang, S. Liu, R. Ding, R. Kishor, and Y. Zheng, "Single laser pulse generates dual photoacoustic signals for differential contrast photoacoustic imaging," Sci. Rep. **7**(1), 1–12 (2017).
5. M. P. Mienkina, C.-S. Friedrich, N. C. Gerhardt, M. F. Beckmann, M. F. Schiffner, M. R. Hofmann, and G. Schmitz, "Multispectral photoacoustic coded excitation imaging using unipolar orthogonal Golay codes," Opt. Express **18**(9), 9076–9087 (2010).
6. S.-Y. Su and P.-C. Li, "Coded excitation for photoacoustic imaging using a high-speed diode laser," Opt. Express **19**(2), 1174–1182 (2011).
7. T. J. Allen and P. C. Beard, "Pulsed near-infrared laser diode excitation system for biomedical photoacoustic imaging," Opt. Lett. **31**(23), 3462–3464 (2006).
8. T. J. Allen and P. C. Beard, "High power visible light emitting diodes as pulsed excitation sources for biomedical photoacoustics," Biomed. Opt. Express **7**(4), 1260 (2016).
9. T. J. Allen, J. Spurrell, M. O. Berendt, O. Ogunlade, S. U. Alam, E. Z. Zhang, D. J. Richardson, and P. C. Beard, "Ultrafast laser-scanning optical resolution photoacoustic microscopy at up to 2 million A-lines per second," J. Biomed. Opt. **23**(12), 1 (2018).
10. T. J. Allen, S. Alam, E. Z. Zhang, J. G. Laufer, D. J. Richardson, and P. C. Beard, "Use of a pulsed fibre laser as an excitation source for photoacoustic tomography," Proc. SPIE **7899**, 78991V (2011).
11. T. J. Allen, M. O. Berendt, J. Spurrell, S. U. Alam, E. Z. Zhang, D. J. Richardson, and P. C. Beard, "Novel fibre lasers as excitation sources for photoacoustic tomography and microscopy," in *Proceedings of SPIE*, A. A. Oraevsky and L. V. Wang, eds. (2016), Vol. 9708, p. 97080W.
12. M.-Y. Cheng, Y.-C. Chang, A. Galvanauskas, P. Mamidipudi, R. Changkakoti, and P. Gatchell, "High-energy and high-peak-power nanosecond pulse generation with beam quality control in 200-μm core highly multimode Yb-doped fiber amplifiers," Opt. Lett. **30**(4), 358 (2005).
13. H. Zhang, X. Shen, D. Chen, C. Zheng, P. Yan, and M. Gong, "High energy and high peak power nanosecond pulses generated by fiber amplifier," IEEE Photonics Technol. Lett. **26**(22), 2295–2298 (2014).
14. M. Berendt, S. Alam, M. Pal, M. Saha, R. Sen, and D. J. Richardson, "Single Polarization, High Energy Pulsed Fiber Laser from 200 μm Core Yb-Doped Fiber," in *Conference on Lasers and Electro-Optics* (OSA, 2016), p. STh4O.5.
15. E. Zhang, J. Laufer, and P. Beard, "Backward-mode multiwavelength photoacoustic scanner using a planar Fabry-Perot polymer film ultrasound sensor for high-resolution three-dimensional imaging of biological tissues," Appl. Opt. **47**(4), 561–577 (2008).
16. N. Huynh, O. Ogunlade, E. Zhang, B. Cox, and P. Beard, "Photoacoustic imaging using an 8-beam Fabry-Perot scanner," Proc. SPIE **9708**, 97082L (2016).
17. B. E. Treeby and B. T. Cox, "k-Wave: MATLAB toolbox for the simulation and reconstruction of photoacoustic wave fields," J. Biomed. Opt. **15**(2), 021314 (2010).
18. N. T. Huynh, O. Francies, K. Soteriou, T. Allen, K. Pham, S. Noimark, S. bodian, A. Desjardins, J. Zhu, O. Abeyakoon, F. Kuklis, E. Zhang, B. Cox, A. Plumb, and P. Beard, "High resolution 3D photoacoustic scanner for clinical vascular imaging applications (Conference Presentation)," in *Photons Plus Ultrasound: Imaging and Sensing 2020*, A. A. Oraevsky and L. V. Wang, eds. (SPIE, 2020), Vol. 11240.
19. T. J. Allen, E. Zhang, and P. C. Beard, "Fully parallelised read-out of a Fabry-Perot ultrasound sensor using an InGaAs camera for fast photoacoustic imaging (Conference Presentation)," in *Photons Plus Ultrasound: Imaging and Sensing 2020*, A. A. Oraevsky and L. V. Wang, eds. (SPIE, 2020), Vol. 11240.
20. X. L. Deán-Ben and D. Razansky, "Optoacoustic signal excitation with a tone-burst of short pulses," Photoacoust. **11**, 1–5 (2018).
21. M. Mienkina, C.-S. Friedrich, N. Gerhardt, W. Wilkening, M. Hofmann, and G. Schmitz, "Experimental evaluation of photoacoustic coded excitation using unipolar golay codes," IEEE Trans. Ultrason., Ferroelect., Freq. Contr. **57**(7), 1583–1593 (2010).
22. M. P. Mienkina, A. Eder, G. Schmitz, C.-S. Friedrich, N. C. Gerhardt, and M. R. Hofmann, "Simulation study of photoacoustic coded excitation using Golay Codes," *2008 IEEE Ultrason. Symp.* 1242–1245 (2008).
23. H. K. Zhang, K. Kondo, M. Yamakawa, and T. Shiina, "Coded excitation using periodic and unipolar M-sequences for photoacoustic imaging and flow measurement," Opt. Express **24**(1), 17 (2016).
24. A. Mandelis, "Time-delay-domain and pseudorandom-noise photoacoustic and photothermal wave processes: a review of the state of the art," IEEE Trans. Ultrason., Ferroelect., Freq. Contr. **33**(5), 590–614 (1986).
25. A. Forbrich, P. Shao, W. Shi, and R. J. Zemp, "Lifetime-weighted photoacoustic imaging," J. Opt. **18**(12), 124001 (2016).
26. X. Shen, H. Zhang, and M. Gong, "High Energy (100 mJ) and High Peak Power (8 MW) Nanosecond Pulses Delivered by Fiber Lasers and Self-Focusing Analysis Based on a Novel Mode Decomposition Method," IEEE J. Sel. Top. Quantum Electron. **24**(3), 1–6 (2018).